ChemComm

Accepted Manuscript

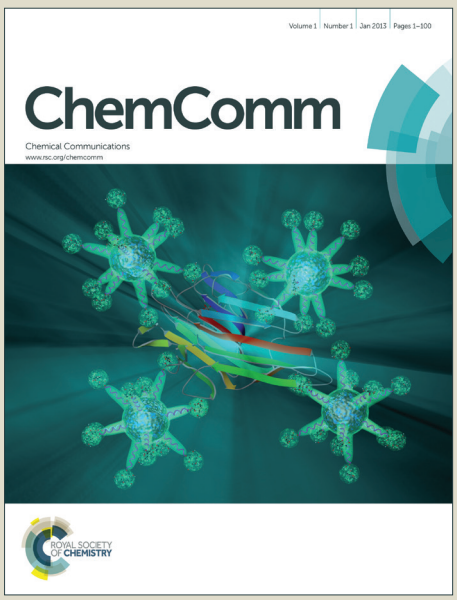

ROYAL SOCIETY OF CHEMISTRY

www.rsc.org/chemcomm

Journal Name

RSCPublishing

COMMUNICATION

Engineering Supramolecular Organic Frameworks (SOFs) of *C*-alkylPyrogallol[4]arene with Bipyridine-based Spacers

Cite this: DOI: 10.1039/xoxxoooooox

Received ooth January 2012,
Accepted ooth January 2012

DOI: 10.1039/xoxxoooooox

www.rsc.org/

Rahul S. Patil,[a] Harshita Kumari,[a] Charles L. Barnes[a] and Jerry L. Atwood*[a]

Supramolecular organic frameworks (SOFs) based on pyrogallol[4]arene and 4,4'-bipyridine-type spacer molecules have been investigated. The hydrogen bonding pattern and molecular arrangement in the crystal structures are engineered through the cocrystallization approach. The length of the spacer molecules and the *C*-alkyl tail length of the PgC macrocycle are tuned to influence the hydrogen bonding pattern and thus the overall architecture of the resultant SOFs. Combined solid-state thermal analysis and solution-phase ^{1}H NMR results indicate the amount of solvent loss and the stability of the SOFs in solution.

Subclasses of porous, crystalline organic frameworks, namely, covalent organic frameworks (COFs) and supramolecular organic frameworks (SOFs) have gathered much attentionbecause of their lucrative application in the areas of selective gas sorption/separation,[1-3] catalysis,[4] and electronics.[5] SOFs are the result of complementary interaction of two or more components in a desired thermodynamically favourable fashion through non-covalent interactions. The type of non-covalent supramolecular interaction, such as hydrogen bonds, halogen bonds, cation-π, π-π, or van der Waals, depends on the shape and functional groups of the components that form a SOF. In recent times, considerable effort has been put into the development of novel organic frameworks tailored through non-covalent interactions. In the broad category of SOFs, subclasses of calix[4]arenes, resorcin[4]arenes (RsC) and pyrogallol[4]arenes (PgC) are proven to be useful because of their unique bowl shape and upper rim functionality. The supramolecular frameworks of RsC and PgC with organic molecules have been characterized in order to understand host-guest interactions,[6-8] molecular recognition,[9, 10] and encapsulation of a guest within discrete capsules.[11, 12]

The bowl of an RsC macrocycle has eight hydroxyl groups, whereas that of a PgC macrocycle has twelve hydroxy groups at the upper rim, which makes the upper rim more hydrophilic. In both cases, four *C*-alkyl chains radiate from each of the four linker carbon atoms of the RsC-/PgC-[4]arene constituting the hydrophobic lower rim of the macrocycle. Thus, the crystallization of these macrocycles in a variety of different solvents leads to the formation of either infinite 2D bilayers or hydrogen bonded hexameric/dimeric capsules consisting of six/two bowls, respectively.[11, 13-16] For example, RsC forms a discrete hexamer of six RsC molecules, aided by the presence of eight water molecules. The assembly is held together by sixty hydrogen bonds.[17] On the other hand, PgC forms a comparatively more stable hexamer in the absence of water molecules, with the additional twelve hydrogen bonds due to the extra four hydroxyl groups on the upper rim of each macrocycle.[11, 18] The geometry of an hexameric nanocapsule or that of a bilayer arrangement is the result of intermolecular O-H•••O hydrogen bonds between the hydroxyl groups of the macrocycles. The formation of H-bonded hexameric or dimeric architectures depends on the *C*-alkyl tail length of the macrocycle used and the solvent system used for the crystallization. Most of the supramolecular studies of PgC have focused on encapsulation of guest(s) within these hexameic or dimeric capsules, or within the bilayered arrangement of PgC macrocyles.[11, 14, 19-23] Few attempts have been directed towards the breaking of conventional hydrogen-bonded hexameric or bilayer arrangements of PgC, followed by the construction of unique frameworks, such as metal-seamed dimers and/or hexamers,[24-26] nanotubes,[27] and nano containers.[14] In a recent study, we reported the supramolecular frameworks resulting from the RsC macrocycle with bpy molecules. RsC-bpy type frameworks consist of novel architectures ranging from a discrete capsule to 2D wave-like arrangements.[28] The bpy-type molecules acted as spacer molecules between RsC building blocks that led to the formation of crystalline framework with solvents enclosed within void spaces. The void spaces are either discrete cavities or continuous channels, depending upon the type of spacer molecule, the solvent, and the conformation of the RsC macrocycle.

In this contribution, we utilize the cone shape of the PgC macrocyle with four additional hydroxy groups to construct H-bonded PgC-bpy based crystalline frameworks. SOFs of *C*-propylpyrogallol[4]arene, PgC3, and *C*-methylpyrogallol[4]arene, PgC1, with two bpy type spacer molecules namely,4,4'bipyridine, bpy, and 1,2- Bis (4-pyridyl)acetylene, bpa, are synthesized and characterized using single-crystal X-ray diffraction studies (Scheme 1). In addition, thermogravimetric analysis (TGA) and ^{1}H NMR analysis are performed to deduce the desolvation and stability of these cocrystals.

Macrocycles PgC1[29] and PgC3[29] were synthesized with the acid catalysed condensation reaction of pyrogallol with aldehydes. Similarly, bpa[30] was synthesized using standard procedure available in the literature. The equimolar solutions of PgC and spacer molecules in acetonitrile or an acetonitrile/toluene mixture were prepared. The resultant solutions were mixed in 1:2 molar ratios to obtain colourless solution which yielded single crystals suitable for analyses by slow evaporation within 8-10 days.

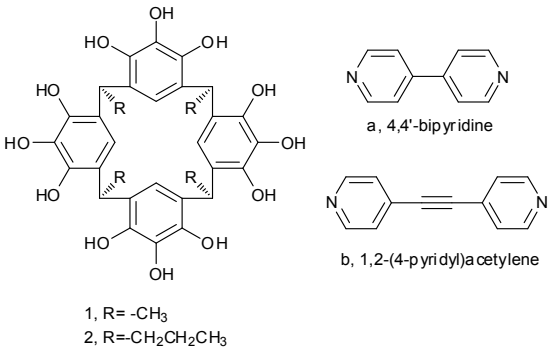

Scheme 1: Components of SOFs

The crystallization of PgCn (n=1, 3) macrocycles in acetonitrile (MeCN) results in the formation of hydrogen bonded network/arrangement (**1**).[15, 16] This network consists of four intramolecular hydrogen bonds between the upper rim hydroxyl groups which are responsible for holding the perfect cone geometry of the macrocycle. The remaining hydroxy groups then form intermolecular hydrogen bonds with the neighbouring PgC macrocycles. The intermolecular hydrogen bonding between macrocycles is either direct hydroxyl-to-hydroxy (PgC1) or assisted through residual water molecules (PgC3).[15, 16] Thus, both PgC1 and PgC3 macrocycles form hydrogen bonds with six neighboring macrocycles in their respective crystal structure (Figure 2, **1**).[15, 16]

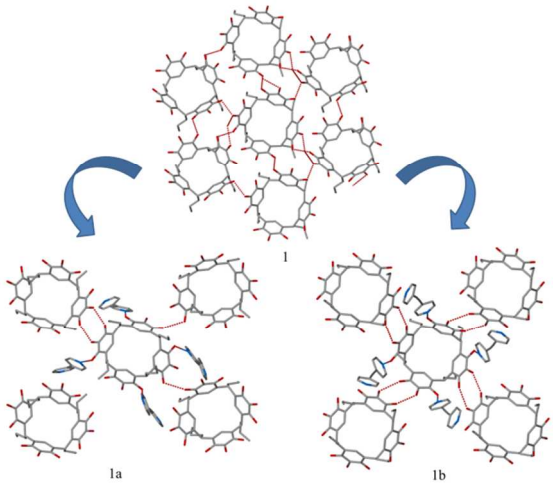

Figure 1. Crystallographic view (001) of hydrogen bonding pattern in **1**, **1a**, and **1b**. Colour codes: C: grey, O: red, N: blue. Hydrogen atoms have been removed for clarity. Figures are not to scale.

The change in this typical intermolecular hydrogen bonding scenario is observed when PgC3 is cocrystallized with the bpyspacer in acetonitrile to form **1a**. **1a**[(PgC3).(bpy).(MeCN)] consist of one PgC3 macrocycle, which forms hydrogen bonds with four bpy molecules as well as with three inverted PgC3 macrocycles. (Figure 1, **1a**) The crystalline framework of **1a** is isostructural with previously reported structure by Atwood et al; however, the solvent used was acetone instead of acetonitrile.[14] The asymmetric unit of **1a** consists of one PgC3, two bpy and one acetonitrile molecule. Symmetry expansion of **1a** reveals that the PgC3 macrocycle hydrogen bonds with three inverted PgC3 macrocycles through four O-H•••O (2.72 Å-3.01 Å) interactions and with four vertically oriented bpy molecules through O-H•••N (2.67 Å-2.81 Å) bonds. Thus, out of eight intermolecular hydrogen bonds in PgC3 crystal/(**1**), four were replaced by O-H•••N interaction with foreign bpy molecules to yield **1a**. The other end of these four bpy molecules form O-H•••N hydrogen bonds with three inverted PgC3 leading to a 2D wave-like hydrogen bonding pattern. The overall framework consists a typical AB bilayer arrangement of PgC3 molecules mediated by O-H•••O interactions and a 2D wave-like arrangement of PgC3 and bpy molecules mediated by O-H•••N interactions. One acetonitrile molecule in the asymmetric unit is situated within the PgC3 bowl forming a CH•••π interaction. Crystallographic expansion of **1a** along (001) crystallographic axis reveals the formation of channels filled with bpy molecules. These channels are constituted of four columns of head to tail arranged PgC3 macrocyles. (Figure 2, **1a**)

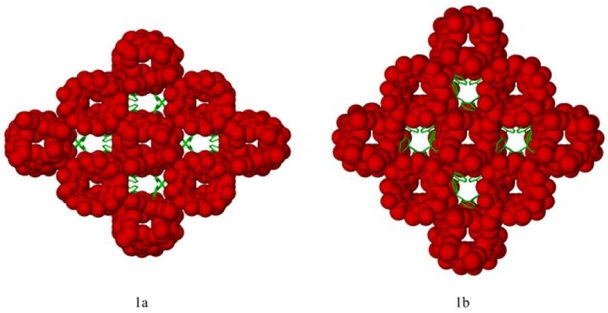

Figure 2. Arrangement of spacer molecules in the channel walled by the stack of tail to head arranged PgC3 in **1a** and **1b**. Colour codes: PgC1/PgC3: red, bpy/bpa: green.Hydrogen atoms have been removed for clarity.

In addition to bpy, the longer spacer molecule (bpa) was tested with PgC3 and an acetonitrile/toluene mixture to obtain the novel crystalline framework of **1b**[(PgC3).(bpa).(MeCN.toluene)]. In case of **1b**, both toulene and acetonitrile solvent molecules, are situated in the channel space within the two head-to-tail arranged PgC3 molecules. Unlike **1a**, wherein each bowl H-bonds with three inverted PgC3s, in **1b** each bowl H-bonds with four inverted PgC3 macrocycles (O-H•••O: 2.69 Å - 2.85 Å). However, in a similar fashion to bpy in **1a**, **1b** has four bpa forming four O-H•••N (2.62Å-2.67Å) hydrogen bonds with one PgC3 (Figure 1, **1a** and **1b**). Each of the four bpa molecules are slightly tilted and the other end of these divergent bpa molecules interacts with four other inverted PgC3 macrocycles though O-H•••N H-bonds. This results in the formation of a 2D wave-like hydrogen bonding pattern between PgC3 and bpa molecules. Thus, similar to **1a**, **1b** also has two type of hydrogen bonding patterns i.e. bilayer arrangement of PgC3 and 2D wave-like arrangement of PgC3 and bpa molecules, resulted from O-H•••O and O-H•••N interactions, respectively. Again, crystallographic expansion of **1b** showed that bpa spacer molecules occupy the space between four columns of head to tail arranged PgC3 macrocycles. (Figure 2, **1b**)

Besides the length of spacer (bpy and bpa), the effect of alkyl tail length (PgC1 vs. PgC3) on the formation of pyrogallol[4]arene-bpy based frameworks was also investigated. Analogous synthesis of PgC1 with bpa and bpy resulted in the formation of **2a**[(PgC1).(bpy).(MeCN)] and **2b**[(PgC1).(bpa).(MeCN)]. Note that unlike **1b** a toluene:acetonitrile mixture was not used in the synthesis of **2b**.

The PgC1 and PgC3 macrocycle exists in two slightly different conformers: a perfect cone with C_{4v} symmetry or a pinched cone with C_{2v} symmetry. The degree of pinching is measured by the centroid-to-centroid distances between the opposite facing pyrogallol rings within the PgC macrocycle. The crystalline framework of **2a**[(PgC1).(bpy).(MeCN)] consists of a perfect cone shaped PgC1 bowl with centroid-to-centroid distance of 6.90 Å. In contrast, PgC1 with bpa/**2b** and PgC3 with bpy/**1a** and bpa/**1b** are slightly pinched with centroid-to-centroid distances of 6.27 and 7.22 (**2b**), 6.56 and 7.10 (**1a**) , 6.75 and 6.84 (**1b**) and, respectively.

Each hydroxyl in the cone is hydrogen bonded to eight bpy molecules through eight O-H•••N (2.73Å-2.74Å) interactions. (Figure 3b) Each PgC1 forms four O-H•••O intramolecular and eight O-H•••N intermolecular hydrogen bonds. Thus, PgC1 forms four additionalO-H•••N intermolecular interactions compared to PgC3. This arrangement completly eliminates the formation of eight intermolecular O-H•••O hydrogen bonds observed otherwise, in case of PgC3. In **1a** and **1b**, both spacer molecules were unable to replace all eight O-H•••O interactions, which was achieved in **2a**. These eight bpy molecules are slightly tilted over the macrocycle and the other end of these bpy molecules hydrogen bonds with four inverted PgC1. Thus a pair of bpy molecules connects with two oppositely positioned PgC1 macrocycle, acting as a connector.(Figure 3c) The arrangement of bpy molecules with respect to PgC1 macrocycle encloses a void space within framework. Thus crystallographic expansion of **2a** along (001) axis converts these void spaces into channels filled with disordered acetonitrile molecules.(Figure 3d) Unlike **1a** and **1b**, channels formed in the **2a** are supported by both PgC macrocycle and spacer molecules.

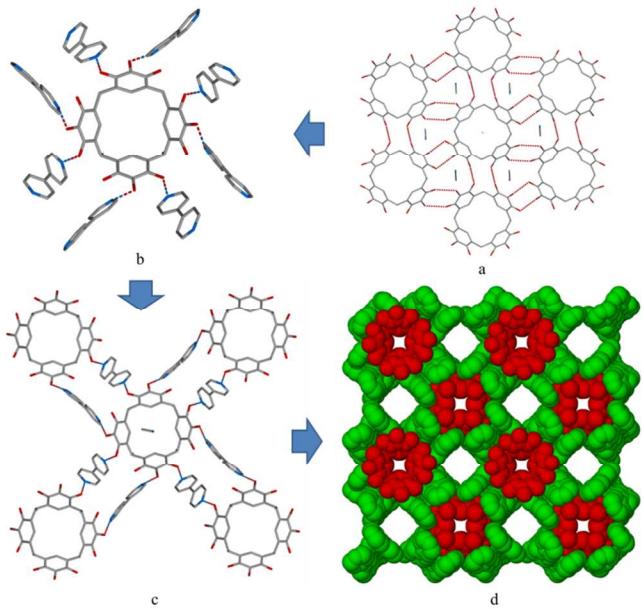

Figure 3.[a] Hydrogen bonding network in PgC1. [b] Arrangement of PgC1 and bpy in **2a**, [c]Two PgC1 connected through two bpy in **2a**, [d] Space filled view of channels formed in **2a**along (001)crystallographic line. Colour codes: C: grey, O: red, N: blue. Hydrogen atoms have been removed for clarity.

The bpa spacer molecule, on the other hand, cocrystallizes with the PgC1 macrocycle, forming **2b**[(PgC1).(bpa).(MeCN)], which exhibits a wave-like arrangement of PgC1 with bpa spacer molecules. Eight hydroxyl groups of the cone shaped PgC1 macrocyle hydrogen bonds with tilted bpa molecules through O-H•••N (2.64Å-2.79Å) interactions. Four out of eight bpa molecules tilt on one side of PgC1 and remaining four tilt towards the other side of the macrocyle. At the other end, these bpa molecules form hydrogen bond with two inverted PgC1 macrocycles on each side of the parent PgC1. Thus four spacer molecules bridges between the two head-to-head oriented PgC1 macrocycles. (Figure 4, **2b**) The exclusive outcome of this hydrogen bonding pattern is a 1D wave-like hydrogen bonding pattern between PgC1 and bpa molecules in the crystalline framework. The intermolecular hydrogen bonding among the macrocycle is absent in this frameworks. The two acetonitrile molecules occupy the space enclosed by two successive hydrogen bonded waves of macrocycle and spacers.

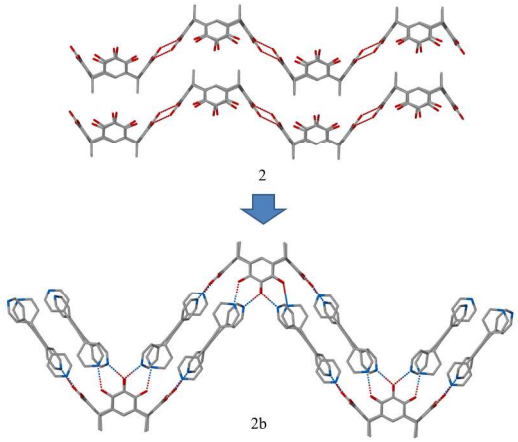

Figure 4. Wave-like arrangement of PgC1 with and without spacer molecules in 2 and 2b. Colour codes: C: grey, O: red, N: blue. Hydrogen bonds have been removed for clarity.

The solution and thermal stability of SOFs is assessed using ^{1}H NMR spectroscopy and thermogravimetric analysis (TGA). For the TGA measurements, 2-5 mg of the individual SOF is subjected to a temperature increment of 15 °C to 350°C, with a step increment of 5°C. Both control PgCn (n=1 or 3) macrocycle as well as SOFs reveal the decomposition of these crystalline material ~220°C, irrespective of the type and number of solvent molecules involved. (Figure 5) The amount of solvent present in the crystalline material before TGA analysis is verified by ^{1}H NMR spectroscopy. The acetonitrile solvent peak at 2.06 ppm is seen in all the spectra. (Table 1 in ESI) A total solvent weight loss of 5%-10% is found in the temperature range 120°C-160°C. Post solvent loss, degradation of spacer molecules occur at around 150°C, followed by decomposition of actual macrocycle at ~220°C in all cocrystals.

Besides the number of solvent molecules, the ^{1}H NMR spectra show the stability of the frameworks in d^6-DMSO. In the case of PgC3, 8.05 ppm and 8.59 ppm peaks represent hydroxyls of the macrocycle. These peaks are present in **1a** but clearly absent in **1b** (Figure 6). This reveals the stability of the hydrogen bonded framework in **1b** in d^6-DMSO. The solution stability of **1b** is due to the presence of twelve intermolecular hydrogen bonds, compared to eight in **1a**. In the case of the PgC1 macrocycle, the ^{1}H NMR

spectrum shows a single peak for hydroxyl hydrogens at 8.08 ppm. A similar peak at 8.08 ppm is observed in ^{1}H NMR spectra of **2a** and **2b**, suggesting that the hydrogen bonded frameworks of **2a** and **2b** dissociate upon dissolution in d^6-DMSO.

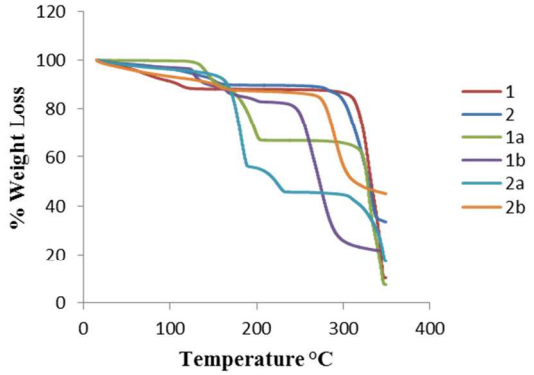

Figure 5: TGA thermograms of SOFs (**1a**, **1b**, **2a**, **2b**) and parent macrocycles (**1, 2**).

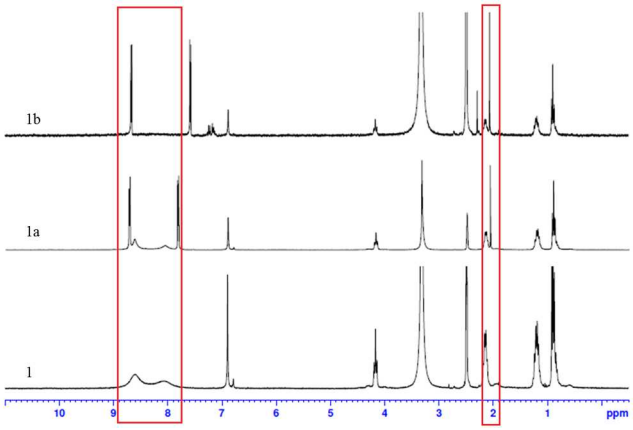

Figure 6.^{1}H NMR spectra of **1**,**1a**, and **1b**showing presence (**1**, **1a)** of and absence (**1b**) of free hydroxyl peaks.

Conclusions

New PgCn-bpy and PgCn-bpa type (n=1, 3) SOFs have been developed by successive breaking of the intermolecular hydrogen bonding within the PgCn macrocyle. The resulting wave-like unique frameworks have channels filled with either solvent or spacer molecules. Of these, only **1b**[(PgC3).(bpa).(MeCN.toluene)] remains intact in solution owing to the presence of four additional H-bonds, evidenced by ^{1}H NMR. SOFs have thermal behaviour distinct from the individual components, and the frameworks are stable post-desolvation, as confirmed by TGA analyses.

Notes and references

Electronic Supplementary Information (ESI) available: CCDC No: 1030566-1030569. [Crystallographic info. and individual TGA graphs of cocrystals are included in ESI]. See DOI: 10.1039/c000000x/

1. L. Chen, P. S. Reiss, S. Y. Chong, D. Holden, K. E. Jelfs, T. Hasell, M. A. Little, A. Kewley, M. E. Briggs, A. Stephenson, K. M. Thomas, J. A. Armstrong, J. Bell, J. Busto, R. Noel, J. Liu, D. M. Strachan, P. K. Thallapally and A. I. Cooper, *Nat. Mater.*, 2014, **13**, 954-960.
2. X. Feng, X. Ding and D. Jiang, *Chem. Soc. Rev.* 2012, **41**, 6010-6022.
3. L.-L. Tan, H. Li, Y. Tao, S. X.-A. Zhang, B. Wang and Y.-W. Yang, *Adv Mater.* 2014, Ahead of Print.
4. S.-Y. Ding, J. Gao, Q. Wang, Y. Zhang, W.-G. Song, C.-Y. Su and W. Wang, *J. Am. Chem. Soc.* 2011, **133**, 19816-19822.
5. S. Wan, J. Guo, J. Kim, H. Ihee and D. Jiang, *Angew. Chem. Int. Ed.* 2008, **47**, 8826-8830.
6. H. Kumari, J. Zhang, L. Erra, L. J. Barbour, C. A. Deakyne and J. L. Atwood, *CrystEngComm*, 2013, **15**, 4045-4048.
7. A. V. Mossine, H. Kumari, D. A. Fowler, A. Shih, S. R. Kline, C. L. Barnes and J. L. Atwood, *Chem. Eur. J.*, 2012, **18**, 10258-10260.
8. L. R. Macgillivray and J. L. Atwood, *NATO Science Series, Series C: Mathematical and Physical Sciences*, 1999, **538**, 407-419.
9. I. Fujisawa, Y. Kitamura, R. Kato, K. Murayama and K. Aoki, *J.Mol. Struct.*, 2014, **1056-1057**, 292-298.
10. I. Fujisawa, Y. Kitamura, R. Okamoto, K. Murayama, R. Kato and K. Aoki, *J.Mol. Struct.*, 2013, **1038**, 188-193.
11. J. Dalgarno Scott, B. Bassil Daniel, A. Tucker Sheryl and L. Atwood Jerry, *Angew.Chemie Int.Ed.*, 2006, **45**, 7019-7022.
12. L. R. MacGillivray, P. R. Diamente, J. L. Reid and J. A. Ripmeester, *Chem.Commun.*, 2000, 359-360.
13. Y. Cohen, L. Avram and L. Frish, *Angew. Chemie Int.Ed.*, 2005, **44**, 520-554.
14. G. W. V. Cave, M. C. Ferrarelli and J. L. Atwood, *Chem. Commun.* 2005, 2787-2789.
15. S. J. Dalgarno, J. Antesberger, R. M. McKinlay and J. L. Atwood, *Chem - Eur. J.*, 2007, **13**, 8248-8255.
16. T. Gerkensmeier, C. Agena, W. Iwanek, R. Frohlich, S. Kotila, C. Nather and J. Mattay, *Zeitschrift fuer Naturforschung, B: Chem. Sci.*, 2001, **56**, 1063-1073.
17. L. R. MacGillivray and J. L. Atwood, *Nature*, 1997, **389**, 469-472.
18. Q.-F. Zhang, R. D. Adams and D. Fenske, *J.Inc. Pheno. Macro. Chem.*, 2005, **53**, 275-279.
19. A. Fowler Drew, J. Teat Simon, A. Baker Gary and L. Atwood Jerry, *Chem.Commun.*, 2012, **48**, 5262-5264.
20. D. A. Fowler, J. Tian, C. Barnes, S. J. Teat and J. L. Atwood, *CrystEngComm*, 2011, **13**, 1446-1449.
21. D. A. Fowler, C. R. Pfeiffer, S. J. Teat, C. M. Beavers, G. A. Baker and J. L. Atwood, *CrystEngComm*, 2014, **16**, 6010-6022.
22. D. A. Fowler, C. R. Pfeiffer, S. J. Teat, G. A. Baker and J. L. Atwood, *Cryst.Growth &Des.*, 2014, **14**, 4199-4204.
23. D. A. Fowler, J. L. Atwood and G. A. Baker, *Chem. Commun.*, 2013, **49**, 1802-1804.
24. S. J. Dalgarno, N. P. Power, J. E. Warren and J. L. Atwood, *Chem.Commun.*, 2008, 1539-1541.
25. N. P. Power, S. J. Dalgarno and J. L. Atwood, *New J. Chem.*, 2007, **31**, 17-20.
26. J. L. Atwood, E. K. Brechin, S. J. Dalgarno, R. Inglis, L. F. Jones, A. Mossine, M. J. Paterson, N. P. Power and S. J. Teat, *Chem.Commun.*, 2010, **46**, 3484-3486.
27. O. V. Kulikov, M. M. Daschbach, C. R. Yamnitz, N. Rath and G. W. Gokel, *Chem.Commun.*, 2009, 7497-7499.
28. R. S. Patil, A. V. Mossine, H. Kumari, C. L. Barnes and J. L. Atwood, *Cryst.Growth &Des.*, 2014, **14**, 5212-5218.
29. F. Weinelt and H. J. Schneider, *J.Org. Chem.*, 1991, **56**, 5527-5535.
30. B. J. Coe, J. L. Harries, J. A. Harris, B. S. Brunschwig, S. J. Coles, M. E. Light and M. B. Hursthouse, *Dalton Trans.*, 2004, 2935-2942.